Prediction of Response to Immune Checkpoint Blockade in Patients with Metastatic Colorectal Cancer with Microsatellite Instability

Alex Duval (alex.duval@inserm.fr)
Sorbonne Université https://orcid.org/0000-0003-1534-1724
Toky Ratovomanana
Sorbonne Université
Remy Nicolle
Université Paris Cité
Romain Cohen
Sorbonne Université, Department of Medical Oncology
Aurélien Diehl
Sorbonne Université and CRSA
Aurélie Siret
INSERM
Quentin Letourneur
Sorbonne Université and CRSA
Olivier Buhard
UMRS 938/INSERM
Alexandre Perrier
Sorbonne Université, Department of Molecular Biology and Genetics
Erell Guillerm
Sorbonne Université, Department of Molecular Biology and Genetics
Florence Coulet
Sorbonne Université, Department of Molecular Biology and Genetics
Raphaël Colle
Sorbonne Université, Department of Medical Oncology
Ada Collura
Sorbonne Université, UPMC Univ Paris 06, Inserm, UMRS 938, Équipe Instabilité des microsatellites et cancer https://orcid.org/0000-0003-0496-1768
Emmanuelle Despras
Sorbonne Université and CRSA
Philippe Le Rouzic
Inserm UMR_S 938, CDR Saint-Antoine, Paris, France

Florence Renaud
Sorbonne Université and CRSA
Agusti Alentorn
Service de Neurologie 2-Mazarin, Sorbonne Université
Mehdi Touat
Service de Neurologie 2-Mazarin, Sorbonne Université
Mira Ayadi
Ligue de lutte contre le cancer https://orcid.org/0000-0002-4019-2858
Pierre Bourgoin
Sorbonne Université and CRSA
Celine Prunier
Saint-Antoine Hospital
Vincent Jonchère
Sorbonne Université and CRSA
Jaafar Bennouna
Centre De Recherche en Cancérologie et Immunologie, Nantes-Angers
Aurélien de Reynies
Université Paris Cité
Jean-François Fléjou
Sorbonne Université and CRSA https://orcid.org/0000-0002-4971-2434
Magali Svrcek
Hopital Saint Antoine,
Thierry André
APHP

Article

Keywords:

Posted Date: May 31st, 2022

DOI: https://doi.org/10.21203/rs.3.rs-1650336/v1

Abstract

Tumors with microsatellite instability (MSI) represent a paradigm for the success of immune checkpoint inhibitor (ICI)-based immunotherapy, particularly in patients with metastatic colorectal cancer (mCRC). To date however, tools for predicting efficacy of these new therapies are lacking. Here we combined high-throughput DNA and RNA sequencing of tumors from 117 patients with MSI mCRC treated with anti-PD-1 +/- anti-CTLA-4 and enrolled into two cohorts, i.e., the NIPICOL clinical trial (NCT03350126) and the ImmunoMSI prospective cohort that were used as discovery and validation cohorts in this ancillary study, respectively. All analyses based on previously suggested DNA/RNA biomarkers of resistance failed to identify robust predictors of treatment response in patients, e.g., the level of MSI, mutational burden, the presence of specific somatic DNA variants as assessed by exome-sequencing and the activity of canonical signaling pathways or the presence of specific cellular contingents within the tumor bulk as estimated by RNA-sequencing. By contrast, resistance to ICI was found to depend both on a small subset of somatic DNA variants located in microsatellite-containing genes with very diverse biological functions and the expression of a stromal-oriented RNA component. Testing of these predictors in 5 large additional independent retrospective and prospective cohorts (IDEA and MOSAIC clinical trials) regrouping 446 patients with nonmetastatic or metastatic MSI CRC untreated with ICI allowed us to validate the specificity of the predictive nature of these indicators regarding ICI-treated MSI mCRC patients. The use of these DNA/RNA predictors will help to refine the ICI-based precision therapy of patients with metastatic MSI mCRC.

Introduction

Mismatch repair deficient (dMMR) tumors display a molecular phenotype characterized by the genetic instability of numerous microsatellite repeated sequences throughout the genome (Microsatellite Instability, MSI) [1–3]. MSI was first observed in inherited tumors associated with Lynch syndrome and later in a large spectrum of primary tumors, in particular sporadic colorectal cancers (CRC) (for review see [4–6]). Being highly genetically unstable, MSI cancers are highly immunogenic and generally show a strong infiltration with cytotoxic T-cell lymphocytes [7]. Recently, it was reported that MSI tumors resist this hostile immune microenvironment by overexpressing immune checkpoint (ICK)-related proteins to allow immune-escape [8]. Consistently, MSI status was shown to predict clinical benefit from ICK inhibitors (ICIs) in patients with metastatic cancer including CRC (mCRC) [9,10]. In patients heavily pretreated with dMMR/MSI mCRC, the objective response rate ranges from 33–65% and the 1-year overall survival rate ranges from 34–71%. First-line pembrolizumab (anti-PD-1) has been associated with significant improvement of progression-free survival compared with standard of care chemotherapy. However, up to 15–46% of patients with dMMR/MSI mCRC exhibit primary resistance to ICIs while 5%-25% of responders develop acquired resistance to these treatments, although this estimation might increase with longer follow-up [11–14].

A few DNA and RNA markers predicting the efficacy of ICIs have been previously proposed in metastatic dMMR/MSI cancer settings [15–22]. However, it is fair to say that these results lack independent validation, being based on the analysis of only limited series of invasive dMMR/MSI tumor samples with heterogeneous tumor origins. At the DNA level, markers include quantitative genomic indexes measuring the level of MSI within the tumor bulk such as MSIsensor or the tumor mutation burden (TMB) whose association to more dense immune infiltration of the cancer in the highly immunogenic dMMR/MSI cancer setting remains uncertain as it has not yet been carefully investigated. Previous studies have considered the selection of specific somatic variants occurring in dMMR cancers due to MSI as specific predictive markers such as *BRAF*^{V600E} mutational status, *KRAS*/*NRAS* mutations, or the B2M truncating mutation resulting in loss of function of the resultant protein associated with the MHC class I complex [17,21]. However, it was recently reported that B2M inactivation was unlikely to blunt the efficacy of ICI in dMMR/MSI tumors in human [23] and using multiple murine dMMR B2m null cancer models [24], raising the question of the real impact of these somatic mutations in the MSI cancer setting. At the RNA level, it was hypothesized that the estimated abundance of some specific cell populations in the tumor microenvironment could be of particular clinical relevance, e.g., some immune cell populations such as antigen-presenting macrophages interacting with T-cells [21]. Logically, deregulated activity of some cancer-related pathways more or less associated with the adaptative T-cell antitumor immunity were also proposed, e.g., the reduced activity of *Wnt/Wingless* signaling, deregulation of the interferon gamma pathway and/or of several immune escape processes [21]. Finally, a study published by our team recently showed that the leading cause for association of primary resistance to ICIs in mCRC was the misdiagnosis of their MSI or dMMR status [25], emphasizing that the first and foremost criteria to be validated before the prescription of ICI in metastatic dMMR/MSI cancer patients, and particularly in mCRC, is the guarantee of a quality diagnosis with appropriate methods to identify genuine dMMR/MSI.

In this study, we addressed the issue of response to ICIs based on two independent prospective cohorts of 44 and 73 patients with dMMR/MSI mCRC, respectively the multicentric NIPICOL clinical trial (NCT03350126) and the prospective ImmunoMSI cohort [26]. Following central reassessment for dMMR/MSI status using gold standard methods to discard misdiagnosed mCRC cases, combined DNA and RNA sequencing of the tumor tissues from these patients was performed. Following supervised analysis of the molecular profiles data which failed to confirm previously proposed DNA/RNA indicators for response to treatment, the use of innovative methods allowed us to identify robust independent DNA and RNA signatures for predicting resistance to ICI. Testing of several retrospective and prospective cohorts (IDEA [27] and MOSAIC [28] clinical trials) regrouping 446 patients with metastatic or nonmetastatic MSI CRC untreated with ICI was also performed to evaluate the specificity of the predictive nature of these indicators, i.e., in the context of immune checkpoint blockade therapy.

Results

Patient population and study design

A total of 130 prospectively collected mCRC patients were assessed for eligibility, including 57 patients from the NIPICOL clinical trial (C1, NCT03350126) and 73 patients from the prospective ImmunoMSI cohort (C2) [26]. Clinical and disease characteristics of patients from C1 and C2 are summarized in **SUPPLEMENTARY TABLE S1** and **SUPPLEMENTARY TABLE S2**. In C1, the analysis was restricted to 54 patients after removing 3 mCRC samples with misdiagnosed dMMR/MSI status. Whole Exome Sequencing (WES) and RNA Sequencing (RNASeq) were performed on 23 and 44 collected mCRC +/- matched normal colonic mucosa paraffin-embedded samples, respectively, after removing 29 samples with lack of materials and/or insufficient quality (Fig. 1A). In C2, targeted next-generation-sequencing (NGS) and RNASeq were performed on 66 and 73 mCRC +/- matched normal colonic mucosa paraffin-embedded samples, respectively, after removing unqualified samples for similar reasons, i.e., insufficient quantity and/or low-quality level (Fig. 1A). The CONSORT-like clinical and molecular diagram in FIGURE 1 outlines the methodology workflow of the study.

FIGURE 1 also summarizes the flow chart (Fig. 1A) and the current design of the study (Fig. 1B). In an effort to optimize the available clinical data for the purpose of identifying available RNA/DNA predictive markers of resistance to ICI in this unprecedent prospective series of ICI-treated patients with MSI mCRC, their putative clinical relevance was examined in both the C1 and C2 cohorts independently. Were considered as clinically relevant the predictors whose status was significantly associated with ICI resistance in C1 and yet in C2, using progression-free survival (PFS) by iRECIST (RECIST for Response Evaluation Criteria in Solid Tumor) criteria for survival analyses (iPFS) [29]. In FIGURE 1 is also indicated how the bioinformatics analyses were carried out. In particular, we indicate how, following analyses of the WES and RNAseq profiles, using previously proposed markers of ICI resistance: (i) we developed a classifier from C1 to predict resistance to ICI in mCRC based on specific combinations of somatic variants occurring in a large panel of microsatellite-containing genes and then validated this classifier in the C2 validation dataset; (ii) we unraveled the phenotypic diversity of mCRC by applying an unsupervised ICA (Independent Component Analysis) on C1 tumor transcriptomes to identify RNA signatures that would be associated with treatment resistance in this discovery dataset and then validated in the C2 validation dataset. Finally, in an effort to validate that both the identified DNA and RNA signatures were truly predictive of response to ICI in patients with MSI CRC, we validated the absence of impact of both these signatures on the survival of patients issued from several prospective and retrospective additional cohorts of MSI CRC untreated with ICI, i.e., in the METAMSI (metastatic MSI CRC, retrospective) [25], IDEA [27], MOSAIC [28] (nonmetastatic MSI CRC, prospective, clinical trials), TIMSI and TCGA (nonmetastatic MSI CRC, retrospective) cohorts (see also materials and methods section for further details) (Fig. 1B).

The level of MSI and TMB in tumor DNA does not predict response to ICI in patients following exclusion of ICI-treated mCRC with misdiagnosed dMMR/MSI status

We first focused DNA analyses on the genomic quantitative indexes that are related to MSI in tumor DNA, i.e., the TMB and MSIsensor score, whose level was previously reported to predict response to ICI in patients with metastatic dMMR tumor [15,16]. FIGURE 2A shows the levels of TMB and MSIsensor score in

the C1 cohort when assessing their level on the basis of WES data. Expectedly, these indexes were highly correlated to each other (Fig. 2A and **SUPPLEMENTARY FIGURE S1**). In this clinical trial (C1 cohort), we previously reported misdiagnoses in 3 patients included in NIPICOL (false positive MSI cases with MSI-PCR and/or IHC, i.e., TN1, TN2, TN3, detected here with negative MSIsensor score, expectedly) [25] and a lack of sensitivity of the MSIsensor tool to detect this tumor phenotype in 3 other patients (false negative MSS cases, FN1, FN2, FN3) [30]. FIGURE 2A shows the TMB and MSIsensor index values in samples from C1 (left panel), including FN and TN cases, together with their MSICare score (right panel) whose higher performance to detect MSI in CRC from their NGS profiles has been recently underlined [30].

Taking into account such diagnostic corrections is crucial and drastically changes the prognostic value that TMB and MSIsensor score have in subsequent survival analyses, expectedly. For instance, we here show that the MSIsensor score displays a statistical tendency of predictive value for the resistance to ICI before correction of diagnostic errors in C1, whereas this same index has no longer any predictive value after correction (exclusion of the 3 false positive MSI cases) (Fig. 2B). Likewise, while a trend for a predictive value of TMB is observed before correction of the same diagnostic errors in C1, this is no longer the case at all thereafter (Fig. 2B). In view of these results, we decided not to investigate further the clinical relevance of TMB and MSIsensor score in C2 since none of them were associated with patients'prognosis in a true MSI mCRC population. As shown in **SUPPLEMENTARY FIGURE S2**, the MSICare score is no more clinically relevant for predicting response to ICI in patients with confirmed MSI mCRC.

No evidence for the relevance of somatic DNA variants predicting MSI mCRC patients' iPFS to ICI

Next, we examined the impact of somatic variants occurring in true positive MSI mCRC patients from C1 regarding response to ICI. Expectedly, a great number of variant-containing genes occurred at both nonrepetitive (NR, in n = 3,886 genes, only coding events) or repetitive (R, in n = 20,472 genes, both coding or noncoding events) sequences, these genes having or not an expected role in the MSI-driven tumorigenic process (Fig. 2C). These somatic events, both coding and noncoding, were observed at variable frequencies in either repetitive (Fig. 2D) or nonrepetitive sequences (Fig. 2E) in tumor DNA, as previously reported [31]. Overall, MSI-driven somatic events at microsatellites (i.e., mononucleotide repeats) were however mostly associated with the background for instability of MSI in colon tumor cells while a minority of these microsatellite mutations were likely positively or likely negatively selected, as previously reported in other large series of localized MSI colon tumors [31] (Fig. 2D).

In FIGURE 2F are shown the results of univariate cox analyses we performed to identify variants with significant impact on the iPFS of MSI mCRC patients from C1 and C2. These tests were first systematically performed for all detected exome-wide somatic variants in C1. Among them, only events associated with *P*-values ≤ 0.1 were sequenced again using targeted NGS in C2 (n = 362 events including 195 and 167 somatic variants at NR and R sequences; see also the study design of the study Fig. 1). This strategy led us to consider 9 and 22 somatic variants with a significant effect on patients' survival in both cohorts at alpha = 5% and 10%, respectively. With the exception of one, i.e., the microsatellite mutation

affecting of the LncRNA TTN-AS1, none of these association to ICI-treated patients' survival remained significant after FDR correction. A listing of these 22 variants is shown on **SUPPLEMENTARY TABLE S3**. Although we suspect that some of these events are clinically relevant, we concluded that their effect at this stage on ICI-treated MSI mCRC patient outcome remains unclear given the insufficient statistical power. Note that canonic mutations recurrently associated with colon tumor among which some were previously proposed to affect response to ICI, e.g., in *KRAS, BRAF, B2M* and other cancer-related genes, were infirmed as being relevant in C1 and not further investigated in C2 (**SUPPLEMENTARY FIGURE S3**).

Identification of an MSI-driven signature predictive of response to ICIs by monitoring somatic mutations on a selected set of microsatellite sequences by machine learning

Our results suggest that a number of somatic variants in microsatellite-containing genes may be potentially associated with ICI resistance in MSI mCRC, without any of them having a sufficient value alone. In light of these new insights, we hypothesized that response to treatment would be better predicted by considering these potentially influential events together in a single classification model.

From C1 (Training cohort), we trained a supervised binary classifier (Random Forest, RF) considering the relapse status as the dependent variables and the mutational status of the 19 microsatellites whose mutations were identified as being associated with response to treatment using univariate cox model as the independent variables (Fig. 3A). Applying the trained model in C2 (Validation cohort), we were able to show that the same model was significantly associated to iPFS (Fig. 3B). FIGURE 3 also illustrates the two groups of variants whose presence and absence in tumor DNA contribute to predicting resistance to ICI in MSI mCRC patients (see the heatmap on Fig. 3C). In addition, no prognostic impact of the same DNA predictor was detected when examined in the 5 cohorts of patients with MSI metastatic (PFS) or nonmetastatic (DFS, Disease-Free Survival) colorectal cancer untreated with ICI, thus validating the specificity of the predictive nature of this indicator regarding ICI-treated MSI mCRC patients (Fig. 3B).

Supervised RNAseq analysis fails to identify established phenotypic markers associated with response to ICI in MSI mCRC patients

We then sought to evaluate established general phenotypic and cellular marker of response to ICI. Three types of markers were applied to and systematically assessed in both discovery (C1) and validation (C2) cohorts, i.e., signatures quantifying cellular components of the tumor microenvironment, single gene expression levels, and pathway-level estimations of expression. TME (tumor microenvironment) components previously associated to differential response to ICI such as the infiltration levels of T or B lymphocytes, of the monocyte lineage or of fibroblasts could not be reproducibly associated to iPFS in the two ICI-treated MSI mCRC cohorts (Fig. 4A). Similarly, the level of expression of the two targeted immune-checkpoint *PD-1, PD-L1* and *CTLA-4* was not robustly associated to iPFS under immunotherapy. In addition to this focused approach, a systematic screen was applied. A total of 99 RNA signatures of cellular component of the TME were tested encompassing various immune and stromal phenotypes, none of which had a significant association with iPFS in either cohort (FDR 5%) (Fig. 4B and 4E and **SUPPLEMENTARY TABLE S4**). Similar results were obtained with the estimated expression activity of

3,365 pathways (Fig. 4C and 4F). More specifically, gene sets involved in angiogenesis, epithelial-to-mesenchymal transition, related TGF-beta and Wnt/Wingless signaling pathways, as well as TNF, interferon, KRAS or mTOR had either a minor and unreproduced association with iPFS in one cohort but more generally no significant correlation with survival in any of the two ICI-treated MSI mCRC cohorts (**SUPPLEMENTARY FIGURE S4**). Finally, the gene-level expression association (10,515 genes tested) identified 5 genes with significant association to iPFS in C2 with either no association with iPFS in C1 and often an opposite hazard-ratio (Fig. 4D and 4G). Overall, signatures previously established in generic contexts or associated to response to ICI in MSS tumors failed to show any signal in MSI mCRC.

An independent component analysis of the MSI tumor transcriptome predicts ICI resistance in mCRC patients

In order to identify context-dependent RNA signatures, *i.e.*, phenotypic descriptors effectively observable in MSI mCRC, an unsupervised blind source separation approach was applied to the 44 NIPICOL transcriptome profiles (C1). Ten independent components were extracted, four of which were significantly associated to objective response as evaluated by iRECIST in C1 (**SUPPLEMENTARY FIGURE S5**) [29]. Two of these were also associated to shorter iPFS in this cohort of patients treated with a combination of ICI suggesting a long-term predictive value of these signatures. Finally, only one of these was also associated to iPFS in C2 (**SUPPLEMENTARY FIGURE S5**). This signature was associated to a tendon-like phenotype, extracellular matrix (ECM)-producing and interacting genes and was considered as an RNA signature of malignant-associated fibrosis and to be referred to as a stromal signature. The signature was significantly correlated to an RNA-based quantification of fibroblasts ($P < 0.001$) and anti-correlated to the tumor cellularity ($P < 0.001$) confirming its stromal origin (Fig. 5A and **SUPPLEMENTARY FIGURE S6**). A transcriptomic deconvolution model of the consensus molecular subtypes of CRC (CMS1 to CMS4) was applied to C1 identifying most samples as mainly CMS1 (72%) as well as a substantial number of samples as predominantly CMS4 (22%) [32]. The estimated intra-tumoral proportion of CMS4 was significantly anti-correlated with tumor cellularity (R= -0.66, $P < 0.001$), suggesting the estimated intra-tumor CMS4 proportion to be quantifying a stromal phenotype rather than an epithelial tumor phenotype. The stromal signature was also significantly correlated with the intra-tumor CMS4 proportion, suggesting to specifically quantify the stromal counterpart of the CMS4 subtype.

As a continuous score quantifying the level of tumor-associated fibrosis, the signature was significantly associated to iPFS of patients under ICI in C1 (HR = 1.87, 95% CI [1.06–3.3]) and in C2 (HR = 1.75, 95% CI [1.03–2.98]) (Fig. 5B). Kaplan-Meier analyses of the stromal signature and its significant clinical impact regarding response to ICI in patients from C1 and C2 are also shown in FIGURE 5C. To evaluate the specificity of the prognostic value of the stromal signature to ICI-treated patient, the signature was applied to five series of nonmetastatic or metastatic MSI CRC that did not receive ICI (Fig. 5D). The stromal signature was not associated to disease-free survival (DFS) or progression-free survival (PFS) in any of the five series, both in metastatic (PFS) and nonmetastatic (DFS) settings, suggesting a strong specific predictive value of this RNA indicator for the efficacy of immune checkpoint inhibitors in MSI

mCRC. In contrast, none of the CMS signature could be associated to iPFS in both C1 and C2 (**SUPPLEMENTARY FIGURE S6**).

Multivariate Analyses

We finally examined the effect of both RNA and DNA signatures in predicting iPFS to ICI in MSI mCRC patients using a multivariate model (Fig. 6). Either when taking into account both signatures in a continuous or a discrete way, the multivariate analysis indicated that both signatures were independently predictive of iPFS (Fig. 6A). Figures 6B and 6C show how these DNA and RNA signatures are complementary and effective when used together in predicting the response of patients to ICI treatment. In patients in whom both are absent (i.e., group low.low), in 34/66 or 51.5% of cases, only one progression event is observed (risk of relapse 1/34, 3%) whereas the remaining progression events are all detected in patients in whom at least one of the two signatures is present (i.e., group high.low, low.high or high.high, risk of relapse 11/32, 34.4%). Overall, one or another of the signatures is able to predict progression in the majority of patients with disease progression (8/12, 66%) while both the signatures when positive are observed in all but one remaining patients with disease progression (3/12, 25%). This makes these signatures a sensitive classifier tool capable of predicting relapse in almost all patients (only 1 relapse observed in the low.low group), albeit with low specificity.

Discussion

In this study, we examine the issue of response to ICI in patients with MSI mCRC. Two prospective cohorts of patients that are larger than any other in the field are examined to investigate this question. The study is limited to CRC patients only, thus avoiding the risk that the origin of the primary tumor might interfere with the results. The dual approach of high-throughput analysis of tumor DNA and RNA enables us to perform both supervised and unsupervised analyses in the aim of investigating ICI-response associated genotypes and phenotypes. Note worthily, the dMMR/MSI status of the tumors was systematically rechecked in our expert center as part of this ancillary study to avoid misdiagnoses which can deeply impact the findings of such translational research studies, as recently reported [25,33]. Besides, the specificity of the predictive nature of the DNA/RNA indicators we identified regarding iPFS in patients treated with ICI was assessed by examining also their association to survival (PFS or DFS) in several distinct cohorts regrouping several hundreds of patients with MSI metastatic or nonmetastatic colorectal cancer untreated with ICI (i.e, prognostic value versus predictive value). All these points constitute methodological strengths of the present work compared to others in the field which remain few in number and based on smaller number of patients. For these reasons, we believe that our findings are therefore robust and likely to provide a new basis for refining the use of ICI in patients with MSI cancer tomorrow, at least in the metastatic CRC setting and possibly in a more general context.

We first show that several previously suggested indicators are unlikely to have any predictive values regarding response to ICI in MSI mCRC patients. This is primarily the case for the quantitative markers MSIsensor and TMB [15,16]. Our data establish that these markers, which are quantitative and related to the

level of nucleotide instability in tumor cells, no longer seem to have any capacity in the clinic for predicting the response to ICI in patients when the diagnostic errors regarding the MSI status of the tumors are corrected upstream and false positive MSI cases with expected low MSIsensor score and TMB are therefore excluded. These results indicate the importance of rigorously confirming an MSI phenotype before the use of ICI immunotherapy, since as expected, all but one of the false positive MSI cases display early resistance to this treatment. In the future, it will be important to validate these negative results, by continuing to examine the effect of these markers in other series of patients with metastatic MSI tumors treated with ICI, being very vigilant about their dMMR/MSI status at the time of diagnosis, as previously stated [25].

In addition, our analyses based on previously defined candidate DNA/RNA markers of resistance, e.g., the specific somatic DNA variants, the activity of canonical signaling pathways or the presence of specific cellular contingents within the tumor bulk, failed to identify robust predictors of ICI response in patients. Some of these markers may contribute to some extent to modulate the patients' response to ICI in some MSI mCRC, and more generally may be predictive of ICI efficacy in MMR proficient tumors. Nevertheless, their prognostic value and clinical relevance was not confirmed in our cohorts of ICI-treated MSI mCRC. Though one somatic noncoding microsatellite variant in TTNAS1 was statistically confirmed to be of clinical interest, the lack of mechanistic data connecting this event to a specific functional scenario leads to consider this candidate with caution for the moment. Its association with treatment resistance will definitely need to be confirmed in subsequent studies.

In this particular context, the breakthrough results we have achieved in this study stem from the fact that we report two distinct original signatures derived from a more global analysis of the DNA and RNA profiles of ICI-treated MSI mCRC. In brief, the DNA signature analyzes the combination of roughly twenty microsatellite variants whose presence and/or absence predicts response to ICI in patients, aggregating independent somatic events within microsatellite containing-genes associated to distinct biological processes. The reliability of this MSI-driven DNA signature originates from the fact that we validate its clinical impact in the ImmunoMSI cohort following its initial elaboration in the NIPCOL training cohort using machine learning. In addition, an RNA component is also predictive of ICI responses in MSI mCRC patients. This component is stromal in nature. It is complex and involves the expression of a number of genes associated with the extracellular matrix. Several functional hypotheses can be proposed to explain this result, in relation to a rich literature that has already provided evidence that the extracellular matrix and its heterogeneous content could promote resistance to ICI in MSS tumor models associated with various primary locations (for review see [34]). The RNA contingent we are identifying could thus play such a role by promoting, for example, immune-exclusion or sequestration processes in the context of increased fibrosis generated in and around the tumor. It could also modulate the response to treatment through non-mutually exclusive mechanisms involving more specifically the cancer-associated fibroblasts hosted in or responsible for the matrix generation. In the future, it will be important to examine these multiple functional routes by further analyzing the complex nature of this ICI resistant-related stroma in the MSI cancer setting.

Our study has some limitations. It does not shed light on simple and clear mechanisms underlying resistance to ICI in MSI mCRC. In this respect, it is not yet very enlightening for the identification of novel therapeutic targets that could be of interest in the future for patients with primary or secondary resistance to anti-PD-1 ± anti-CTL4. Furthermore, although our results were established on a large prospective collection of patients including two independent cohorts, one of which is a clinical trial, they still require validation in new populations of metastatic MSI cancer patients, with colorectal tumor but possibly also other primary MSI cancer. Despite these weaknesses, the 2 signatures we outline here from the analysis of the tumor bulk are easy to investigate and can be implemented in the context of a clinical routine; the DNA signature requires the analysis of the status of only 19 microsatellite markers within the tumor, ideally by NGS but possibly also by other methods while the RNA signature requires to perform 3'RNA-sequencing which is a simple, reproducible and feasible method to be used with paraffin-embedded tumor samples, the cost of which has now decreased considerably. It is very interesting to note that these two signatures are complementary and primarily detect distinct scenarii of ICI resistance in patients. We thus recommend to use both of them for patients given they have independent predictive value. Here their joint use made it possible to identify a first group of patients whose response to ICI is almost always excellent, in contrast to a second group in which all but one treatment resistance was observed. Such a classification should be of interest for the design of future strategies improving ICI for MSI cancer patients in clinics.

Materials And Methods

Patients

The Nipicol clinical trial (C1) was conducted in accordance with the tenets of the Declaration 170 of Helsinki and Good Clinical Practice Guidelines, after approval by the ethics board, and was registered at ClinicalTrials.gov (Clinical trial number: NCT03350126). Written informed consent was obtained from all patients. Concerning ImmunoMSI prospective cohort (C2), all consecutive MSI/dMMR mCRC patients enrolled in ICI trials (anti-PD-1 monotherapy or the anti-PD-1 plus anti-CTLA-4 combination) or treated with ICI (anti-PD-1 monotherapy) under a compassionate used program at Saint-Antoine Hospital, Medical Oncology department (Prof. Thierry André) from February 2015 to December 2019, were included. This research was approved by the ethics committee (N°2020 – CER 2020-6).

Sample preparation and sequencing

For Nipicol cohort, genomic DNA isolated from formalin- fixed paraffin- embedded (FFPE) were captured using Twist Human Core Exome Enrichment System (Twist Bioscience) + IntegraGen Custom as previously described [35]. For ImmunoMSI cohort, hybridization probes and extension primers were designed using Roche's HyperDesign Tool for NGS Target Enrichment process. Sequence capture, enrichment and elution were performed according to manufacturer's instruction and protocols without modification except for library preparation performed with NEBNext® Ultra II kit (New England Biolabs®).

DNA samples were then sequenced on an Illumina NovaSeq as Paired-end 100 reads. The generated reads were mapped to the reference genome hg38 (GRCh38).

Assessment of microsatellite status

All CRC samples from C1, C2 and other cohorts used in this post-hoc study were centrally reassessed for MSI and dMMR status using immunohistochemistry (IHC) and for MSI using polymerase chain reaction (PCR) as described. Next, MSIsensor (version 0.6) and MSICare were used by default on paired normal-tumor exome data, to evaluate the mutation status of microsatellites using considering the whole exome data. MSIsensor score threshold of 10% or more was used to classify the MSI-H tumor (MSI-High) and a MSICare threshold of 20% was used to define MSI status as previously described [30].

Exome Analysis and Mutational load

Variant calling for the identification of SNVs (Single Nucleotide Variations) and small insertions/deletions (up to 20bp), was performed via the Broad Institute's GATK Haplotype Caller GVCF tool (GATK3.8.1) for constitutional DNA and via the Broad Institute's MuTect tool (2.0, –max_alt_alleles_in_normal_count = 2; –max_alt_allele_in_normal_fraction = 0.04) for somatic DNA. A Fisher's Exact Test is applied after MuTect2 variant calling to improve filtering of variants with strand bias. The tumor mutational burden (TMB) is calculated by dividing the number of somatic mutations by the number of bases having a depth greater than 10. The somatic mutations used for the mutational load were filtered as follows: Somatic score > 3, Mutated Allele Frequency in Tumor tissue ≥ 5%, Mutated Allele Count in Tumor tissue ≥ 3, Mutated Allele Frequency in Constitutional tissue < 4%.

Survival analysis of ICI treated patients

Survival analysis on ICI patients was performed from the date of first infusion of any ICI. iPFS by iRECIST [29] was calculated from the first dose to the first documented PD with subsequent confirmation, or death resulting from any cause, whichever occurred first. Kaplan Meier curves were used to visualize difference in progression free survival (iPFS) between patients' groups diverging on genomic instability (TMB-High or MSISensor-High or MSICare-High,>20th percentile; TMB-Low or MSISensor-Low or MSICare-low ≤ 20th percentile). Log-rank test was performed using the R package Survival (version 3.2.3).

Feature selection and data pre-processing

To face the high dimensionality curse before running a machine learning algorithm on our high dimension dataset (over 279 positions explored) we decided to keep only the positions with a Cox regression *P*-value in Nipicol lower than 0.05 [36]. We also decided to only focus on variations in MS regions.

In order to train a Random Forest (RF) model on our DNA sequencing data, we had process missing sequencing data at certain locations for some patients. Indeed, RF does not support missing data in its learning or prediction. As a result, the missing data must be imputed. However, we have applied a filter to the maximum rate of missing data allowed in a position in Nipicol to avoid the amount of bias introduced

by the imputation. To do so, we firstly calculated this value in other available WES cohorts of MSI CRC, i.e., the public cohort TCGA and two other large private cohorts we have already sequenced and analyzed in the lab (data not shown). This allows us to exclude positions that are generally difficult to sequence. Secondly, we did the same on the Nipicol cohort to exclude the remaining mis-sequenced positions. We have chosen to allow a maximum of 5% of missing data per MS over the external WES or Nipicol.

Once done, we iteratively imputed missing data using the python scikit-learn package [37] which imputes missing values by modeling those as a function of the other non-missing values. We used an Extra Tree regression model for the imputation. Because of the class imbalance in our training cohort (4 non-responder vs. 19 responder) we applied an up-sampling process to balance the two classes and increase the size of the cohort.

Random Forest training and validation

With those filters we selected 19 MS variations of interest on which we trained our RF model. We used the RF model integrated in the python scikit-learn package with 2000 trees.

We used a matrix containing the mutation status for each MS in every Nipicol patient (1 if mutated, 0 else) as the input values and the iPFS status as the binary target values. We obtained a model that was able to predict the progression risk of a patient taking into account its sequencing on the 19 MS investigated.

To validate our model, we predicted the progression risk for each ImmunoMSI patients. Then we ran a Cox regression model to investigate the association between the survival and this new value.

Transcriptome profile generation and analysis

Total RNA was extracted for every tumor sample using QIAGEN Allprep protocol (ref 10.2144/000113829). 150ng of total RNA was used to generate RNAseq sequencing library using Lexogen Quantseq 3’ FWD kit and sequenced by the Institut du cerveau iGenseq plateform on a NovaSeq 6000 aiming for a minimum of 10 million reads. Raw RNAseq reads were mapped to the human genome (Ensembl GRCH38) and Ensembl’s reference transcriptome using STAR. Gene counts were obtained using FeatureCount, normalized by an UpperQuartile procedure and logged on a base 2.

Gene-set definitions of pathways were taken from the Molecular Signature Database (MSigDB v7.5.1) as well as the BioPlanet pathways database (2019) which was downloaded from the EnrichR website. Pathway-level activity was inferred from gene expression levels using the GSVA method with a Gaussian kernel. Based on the ImmuneDeconv evaluation and implementation, five methods for tumor microenvironment quantification were used: XCell, EPIC, Cibersort, MCPcounter and Estimate.

Independent Component Analysis (ICA) was performed on the sample-wise centered gene expression values of the 5,000 genes with the highest average and variable (as measured by standard deviation) expression. The JADE (joint approximation diagonalization of Eigen-matrices) algorithm was applied to

extract 10 components as previously described [38]. The ICA components were projected on other transcriptomic dataset by first selecting genes in common in the reference ICA (computed from the C1 cohort) and in the new transcriptomic dataset. The cross-product of the gene-weight inverted matrix was used as the projection of a new dataset, resulting in 10 scores (one per ICA component) for each new sample.

The intra-tumor proportion of the consensus molecular subtypes of colorectal cancer were estimated using the centroids of the original study [32] and the WISP deconvolution method (cit-bioinfo.github.io/WISP/).

Validation of specific predictive value of genomic and transcriptomic signatures

In order to validate the specificity of the predictive value of both DNA and RNA signatures in MSI mCRC patients treated with ICI, the absence of clinical impact of both these signatures was evaluated in prospective and retrospective additional cohorts of metastatic and nonmetastatic patients with MSI CRC untreated with ICI. We performed Cox survival analyses to examine the METAMSI cohort (retrospective, metastatic MSI CRC: DNA, n = 21; RNA, n = 13), the IDEA cohort (clinical trial, nonmetastatic MSI CRC: RNA, n = 95), the MOSAIC cohort (clinical trial, nonmetastatic MSI CRC: RNA, n = 86), the TIMSI cohort (retrospective, nonmetastatic MSI CRC: DNA, n = 81; RNA, n = 39) and the TCGA cohort (nonmetastatic MSI CRC: DNA, n = 68; RNA, n = 48).

References

1. Ionov, Y., Peinado, M.A., Malkhosyan, S., Shibata, D. & Perucho, M. Ubiquitous somatic mutations in simple repeated sequences reveal a new mechanism for colonic carcinogenesis. Nature **363**, 558–561 (1993).
2. Aaltonen, L.A., *et al.* Clues to the pathogenesis of familial colorectal cancer. Science (New York, N.Y **260**, 812–816 (1993).
3. Fishel, R., *et al.* The human mutator gene homolog MSH2 and its association with hereditary nonpolyposis colon cancer. Cell **75**, 1027–1038 (1993).
4. Collura, A., *et al.* [Microsatellite instability and cancer: from genomic instability to personalized medicine]. Med Sci (Paris) **35**, 535–543 (2019).
5. Hamelin, R., *et al.* [Clinical and molecular consequences of microsatellite instability in human cancers]. Bulletin du cancer **95**, 121–132 (2008).
6. Duval, A. & Hamelin, R. Mutations at coding repeat sequences in mismatch repair-deficient human cancers: toward a new concept of target genes for instability. Cancer research **62**, 2447–2454 (2002).
7. Svrcek, M., *et al.* MSI/MMR-deficient tumor diagnosis: Which standard for screening and for diagnosis? Diagnostic modalities for the colon and other sites: Differences between tumors. Bulletin

du cancer **106**, 119–128 (2019).

8. Llosa, N.J., *et al.* The vigorous immune microenvironment of microsatellite instable colon cancer is balanced by multiple counter-inhibitory checkpoints. Cancer discovery **5**, 43–51 (2015).
9. Le, D.T., *et al.* PD-1 Blockade in Tumors with Mismatch-Repair Deficiency. The New England journal of medicine **372**, 2509–2520 (2015).
10. Colle, R., *et al.* Immunotherapy and patients treated for cancer with microsatellite instability. Bulletin du cancer **104**, 42–51 (2017).
11. Le, D.T., *et al.* Mismatch repair deficiency predicts response of solid tumors to PD-1 blockade. Science (New York, N.Y **357**, 409–413 (2017).
12. Overman, M.J., *et al.* Nivolumab in patients with metastatic DNA mismatch repair-deficient or microsatellite instability-high colorectal cancer (CheckMate 142): an open-label, multicentre, phase 2 study. The lancet oncology **18**, 1182–1191 (2017).
13. Overman, M.J., *et al.* Durable Clinical Benefit With Nivolumab Plus Ipilimumab in DNA Mismatch Repair-Deficient/Microsatellite Instability-High Metastatic Colorectal Cancer. J Clin Oncol **36**, 773–779 (2018).
14. Le, D.T., *et al.* Phase II Open-Label Study of Pembrolizumab in Treatment-Refractory, Microsatellite Instability-High/Mismatch Repair-Deficient Metastatic Colorectal Cancer: KEYNOTE-164. J Clin Oncol **38**, 11–19 (2020).
15. Mandal, R., *et al.* Genetic diversity of tumors with mismatch repair deficiency influences anti-PD-1 immunotherapy response. Science (New York, N.Y **364**, 485–491 (2019).
16. Schrock, A.B., *et al.* Tumor mutational burden is predictive of response to immune checkpoint inhibitors in MSI-high metastatic colorectal cancer. Ann Oncol **30**, 1096–1103 (2019).
17. Gurjao, C., *et al.* Intrinsic Resistance to Immune Checkpoint Blockade in a Mismatch Repair-Deficient Colorectal Cancer. Cancer Immunol Res **7**, 1230–1236 (2019).
18. Chida, K., *et al.* Transcriptomic profiling of MSI-H/dMMR gastrointestinal tumors to identify determinants of responsiveness to anti-PD-1 therapy. Clin Cancer Res (2022).
19. Kwon, M., *et al.* Determinants of Response and Intrinsic Resistance to PD-1 Blockade in Microsatellite Instability-High Gastric Cancer. Cancer discovery **11**, 2168–2185 (2021).
20. Cohen, R., *et al.* Adrenal gland as a sanctuary site for immunotherapy in patients with microsatellite instability-high metastatic colorectal cancer. J Immunother Cancer **9**(2021).
21. Bortolomeazzi, M., *et al.* Immunogenomics of Colorectal Cancer Response to Checkpoint Blockade: Analysis of the KEYNOTE 177 Trial and Validation Cohorts. Gastroenterology **161**, 1179–1193 (2021).
22. Chida, K., *et al.* A Low Tumor Mutational Burden and PTEN Mutations Are Predictors of a Negative Response to PD-1 Blockade in MSI-H/dMMR Gastrointestinal Tumors. Clin Cancer Res **27**, 3714–3724 (2021).

23. Middha, S., *et al.* Majority of B2M-Mutant and -Deficient Colorectal Carcinomas Achieve Clinical Benefit From Immune Checkpoint Inhibitor Therapy and Are Microsatellite Instability-High. JCO Precis Oncol **3**(2019).
24. Germano, G., *et al.* CD4 T Cell-Dependent Rejection of Beta-2 Microglobulin Null Mismatch Repair-Deficient Tumors. Cancer discovery **11**, 1844–1859 (2021).
25. Cohen, R., *et al.* Association of Primary Resistance to Immune Checkpoint Inhibitors in Metastatic Colorectal Cancer With Misdiagnosis of Microsatellite Instability or Mismatch Repair Deficiency Status. JAMA Oncol **5**, 551–555 (2019).
26. Cohen, R., *et al.* RECIST and iRECIST criteria for the evaluation of nivolumab plus ipilimumab in patients with microsatellite instability-high/mismatch repair-deficient metastatic colorectal cancer: the GERCOR NIPICOL phase II study. J Immunother Cancer **8**(2020).
27. Pages, F., *et al.* Prognostic and predictive value of the Immunoscore in stage III colon cancer patients treated with oxaliplatin in the prospective IDEA France PRODIGE-GERCOR cohort study. Ann Oncol **31**, 921–929 (2020).
28. Andre, T., *et al.* Adjuvant Fluorouracil, Leucovorin, and Oxaliplatin in Stage II to III Colon Cancer: Updated 10-Year Survival and Outcomes According to BRAF Mutation and Mismatch Repair Status of the MOSAIC Study. J Clin Oncol **33**, 4176–4187 (2015).
29. Seymour, L., *et al.* iRECIST: guidelines for response criteria for use in trials testing immunotherapeutics. The lancet oncology **18**, e143-e152 (2017).
30. Ratovomanana, T., *et al.* Performance of Next Generation Sequencing for the Detection of Microsatellite Instability in Colorectal Cancer with Deficient DNA Mismatch Repair. Gastroenterology (2021).
31. Jonchere, V., *et al.* Identification of Positively and Negatively Selected Driver Gene Mutations Associated With Colorectal Cancer With Microsatellite Instability. Cell Mol Gastroenterol Hepatol **6**, 277–300 (2018).
32. Guinney, J., *et al.* The consensus molecular subtypes of colorectal cancer. Nature medicine **21**, 1350–1356 (2015).
33. Loupakis, F., *et al.* Prediction of Benefit from Checkpoint Inhibitors in Mismatch Repair Deficient Metastatic Colorectal Cancer: Role of Tumor Infiltrating Lymphocytes. Oncologist **25**, 481–487 (2020).
34. O'Donnell, J.S., Teng, M.W.L. & Smyth, M.J. Cancer immunoediting and resistance to T cell-based immunotherapy. Nat Rev Clin Oncol **16**, 151–167 (2019).
35. Gnirke, A., *et al.* Solution hybrid selection with ultra-long oligonucleotides for massively parallel targeted sequencing. Nat Biotechnol **27**, 182–189 (2009).
36. Polsterl, S., Conjeti, S., Navab, N. & Katouzian, A. Survival analysis for high-dimensional, heterogeneous medical data: Exploring feature extraction as an alternative to feature selection. Artif Intell Med **72**, 1–11 (2016).

37. Abraham, A., *et al.* Machine learning for neuroimaging with scikit-learn. Front Neuroinform **8**, 14 (2014).
38. Puleo, F., *et al.* Stratification of Pancreatic Ductal Adenocarcinomas Based on Tumor and Microenvironment Features. Gastroenterology **155**, 1999–2013 e1993 (2018).

Declarations

ACKNOWLEDGMENTS: The authors thank the patients and their families for making the study possible. The authors acknowledge the GERCOR clinical study teams and investigators and study teams in all centers.

FUNDING: This work was supported by grants from Site de Recherche Intégré sur le Cancer (SIRIC) Cancer United Research Associating Medicine, University & Society (CURAMUS), and the Ligue Nationale Contre le Cancer. T.R was a recipient of a grant from the Region Ile-de-France (PhD Student bursary). Prof. Duval's team has the label de La Ligue contre le Cancer.

AUTHOR CONTRIBUTIONS: study concept and design: TR, RN, Adi, ADu; acquisition of data: TR, RN, RC, Adi, AS, QL, OB, AP, EG, FC, RC, AC, ED, PLR, FR, AA, MT, FB, MA, PB, CP, VJ, JB, AdR, JFF, MS, TA, ADu; analysis and interpretation of data: TR, RN, RC, Adi, ADu; drafting of the manuscript: TR, RN, RC, Adi, ADu; obtained funding; ADu; technical support: TR, RN, Adi, AS, QL, OB, FC, AC, FR, PB, VJ ; study supervision: ADu.

Figures

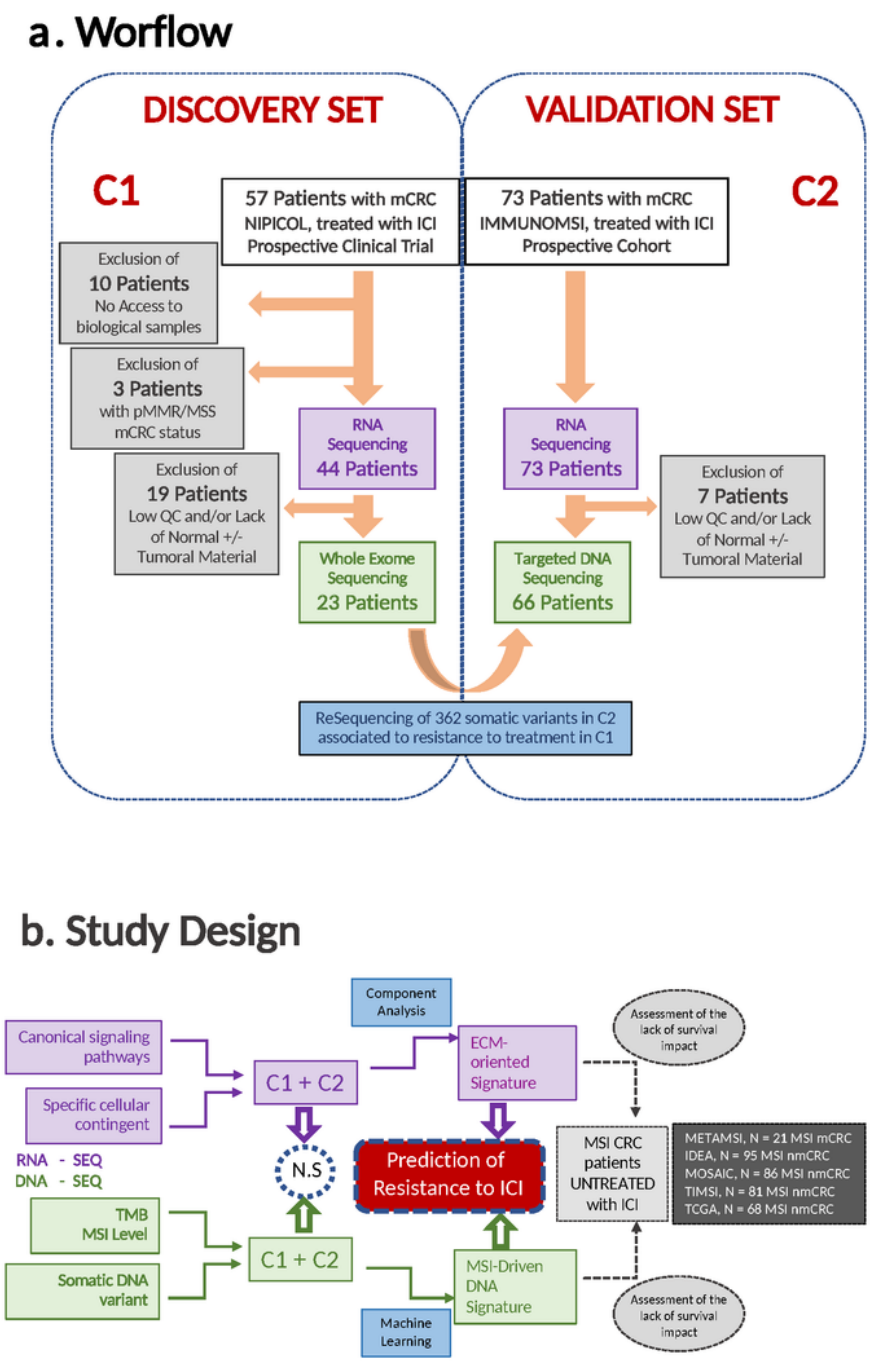

Figure 1

Workflow and Study Design

MSS, microsatellite stable; mCRC, metastatic colorectal cancer; ICI, immune checkpoint inhibitors; IHC, Immunohistochemistry; QC, quality control; pMMR, mismatch repair proficient.

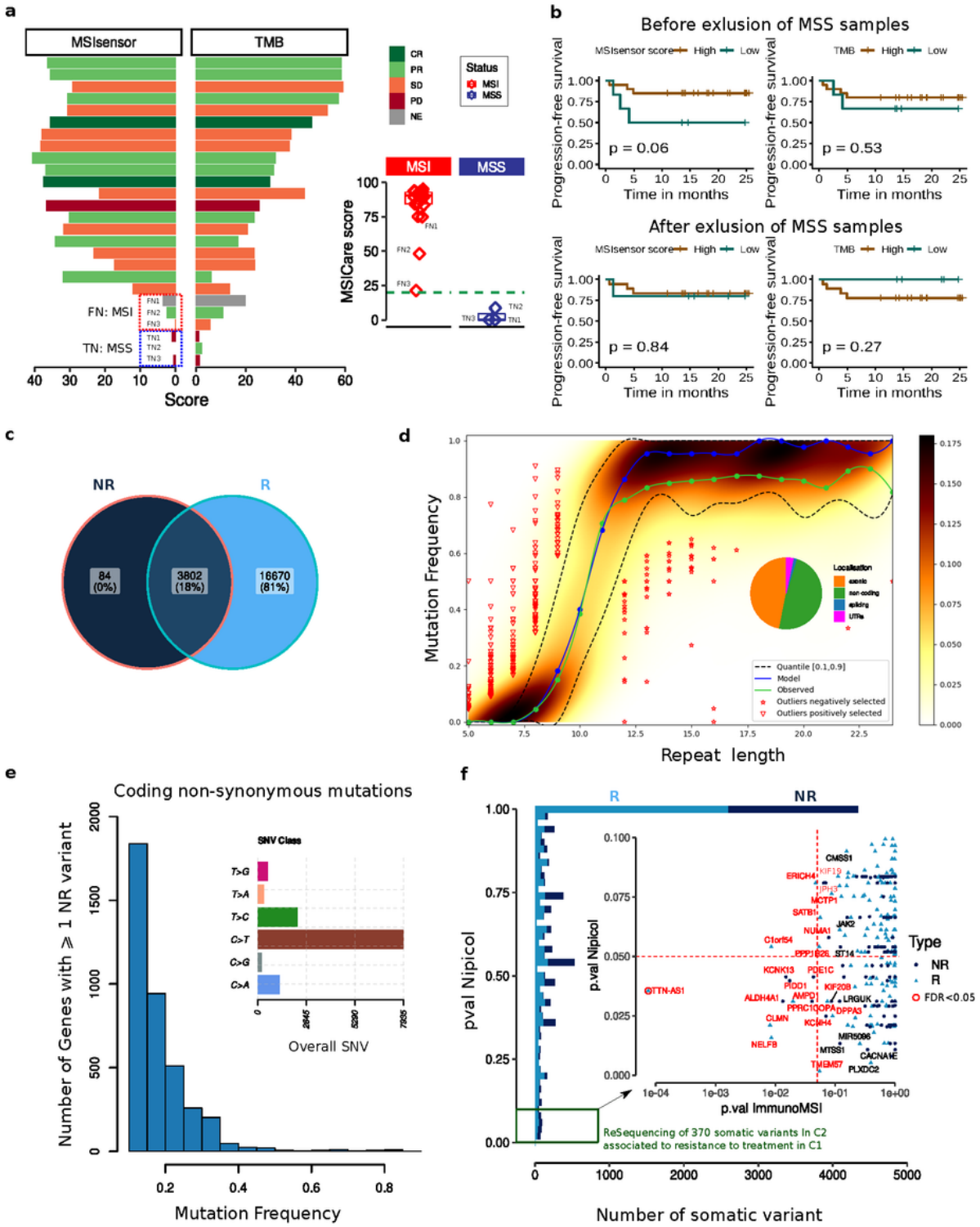

Figure 2

Exome and target sequencing analysis

A) Bar plots show the MSIsensor score and TMB distribution according to iRECIST status of patients (left panel) [29]. Using a MSIsensor score of 10%, false negative dMMR/MSI samples samples from the NIPICOL cohort are framed in red and true negative pMMR/MSS samples are framed in blue. Box plots show the percentage of mutated microsatellites (MSIcare score) according to MSI/MSS status of the tumor samples (left panel). CR, complete response (dark green); PR, partial response (light green); SD, stable disease (orange); PD, progressive disease (dark red).

B) Progression free survival (iPFS) curve before (upper panel) and after (lower panel) exclusion of initially misdiagnosed pMMR/MSS tumor samples. Both for the TMB or for the MSIsensore score, the top 20% are indicated as high (red line) and the rest as low (blue line). For TMB, 20% was chosen because this cutoff optimized the significance of the *P*-value between the two groups.

C) The Venn diagram shows the number and percentage of genes containing non-repeat (NR) and repeat (R) variants.

D) Model of distribution of microsatellite variant frequency across samples according to microsatellite size. The color gradient indicates the density of the b-binomial logistic regression model. The green curve represents the median of the observed mutation frequencies, and the blue curve represents the median obtained from the model. Pie chart indicate the proportion of Microsatellites in exonic (orange), non-coding (green), splicing (blue) and UTRs (pink) regions.

E) Histogram of the number of genes with at least one NR variant according to the mutation frequency of these variants.

F) Histogram of *P*-values from cox analysis for R and NR variants in the C1 Nipicol cohort. A zoom was performed on those having a *P*-value lower than 0.1 after sequencing in the C2 ImmunoMSI cohort. Repeat variants are shown in dark blue and non-repeat variants in light blue. The only variant remaining significant after *P*-value correction in ImmunoMSI is encircled in red. Genes' name of the 22 somatic variants with a significant effect on patients' survival in both C1 and C2 cohorts at alpha=10% are indicated in red.

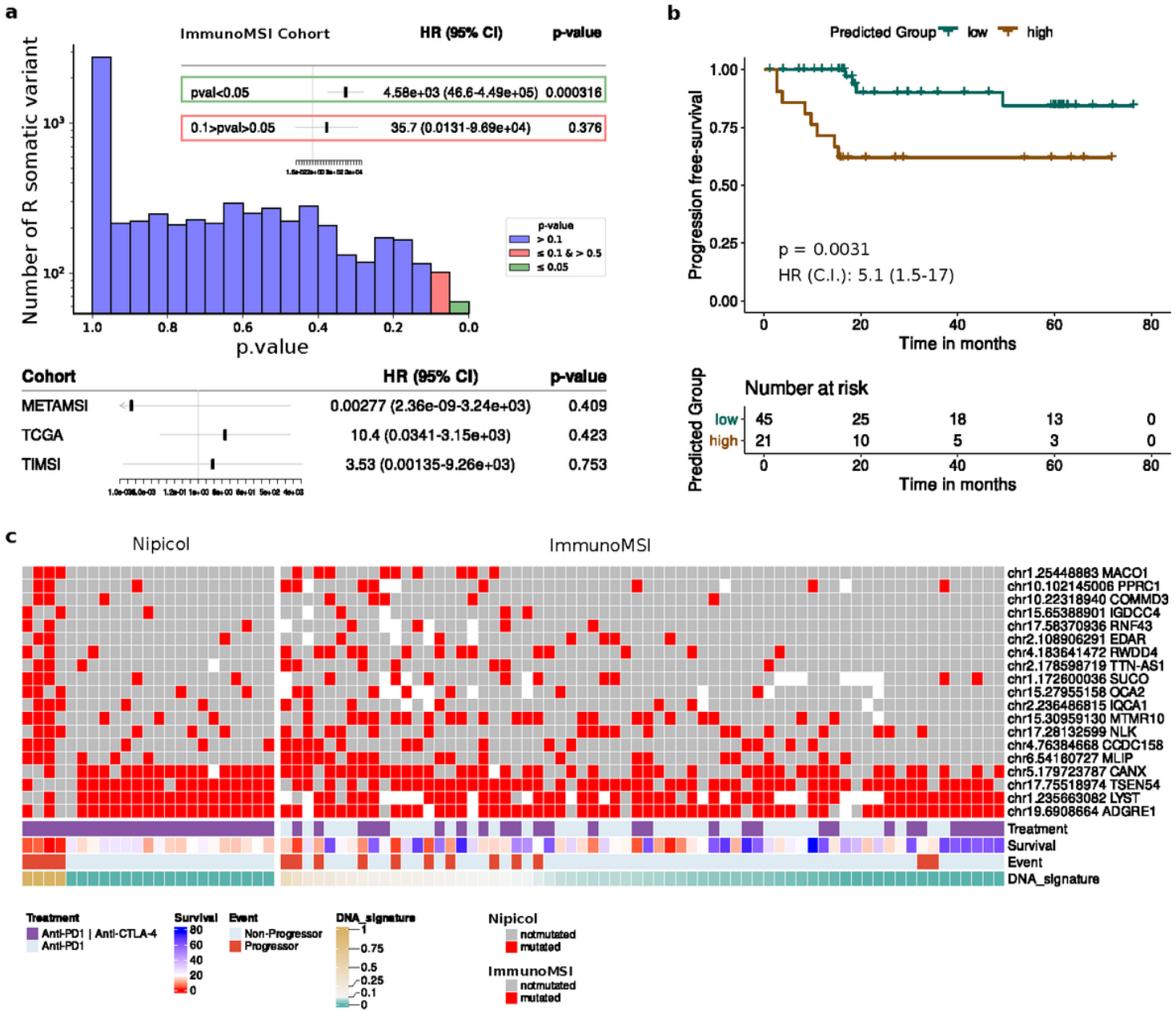

Figure 3

MS selection and random Forest analysis on somatic variants.

A) Counts of microsatellites according to their *P*-value of the uni-variate Cox regression on the 23 patients Nipicol subset. Red and green bar represent the sequenced microsatellites in the validation cohort ImmunoMSI, with respectively a *P*-value < 0.05 and 0.05 ≤ p-value < 0.1. The top forestplot represent the Cox survival regression results on model prediction of risk output. High (P-value < 0.05, DNA signature) in green vs low stringency of Cox features selection based on P-value in red. The bottom forestplot represent the DNA signature with progression-free survival in other cohorts of CRC patients untreated with ICI.

B) Kaplan-Meier curves of iPFS are shown accordingly to risk probability in ImmunoMSI only. Red curve corresponds to patients with low probability (<10%) and blue curve corresponds to patients with high probability (>10%) RF probability. Log-rank test p-value between the group equals 0.00312.

C) Heatmap representation of NIPICOL (C1) and ImmunoMSI (C2). Overview of mutations profile for each patient on the liste of 19 selected microsatellites (MS, see genes' name and chromosomal location on the left). Bottom bars represent their treatment (combo-therapy or mono-therapy), survival (time-to-event), event (Responder or Non-Responder) and DNA.signature (probabilty of non-response given by the RF). Patients are ordered based on predicted risk of progress and MS are ordered in function of mutation frequency in Nipicol cohort.

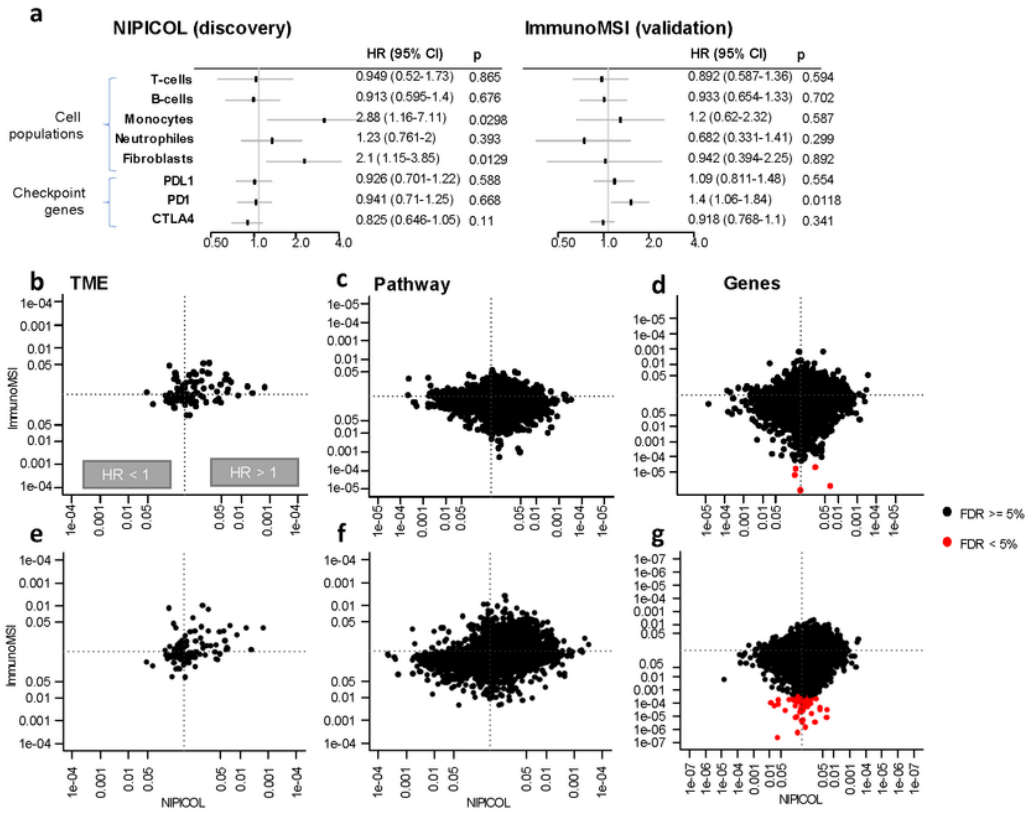

Figure 4

A) Univariate analyses of the association between cell population quantification estimation or single-gene expression levels and the progression-free survival in the two cohorts treated with ICI.

B-G) Distribution of Cox's proportional hazard *P*-value measuring the association of tumor microenvironment signatures (b,e), Pathway's estimated activity (c,f) or single-gene expression levels (d,g) with progression-free survival in C1 and in either the entire C2 (b,c,d) or only in the subset of C2 in which patients received the same combination of ICI than in C1 (e,f,g). In the plots, *P*-values are signed so

that association with increased risk (HR > 1) are positive and association with decreased risk (HR < 1) are negative.

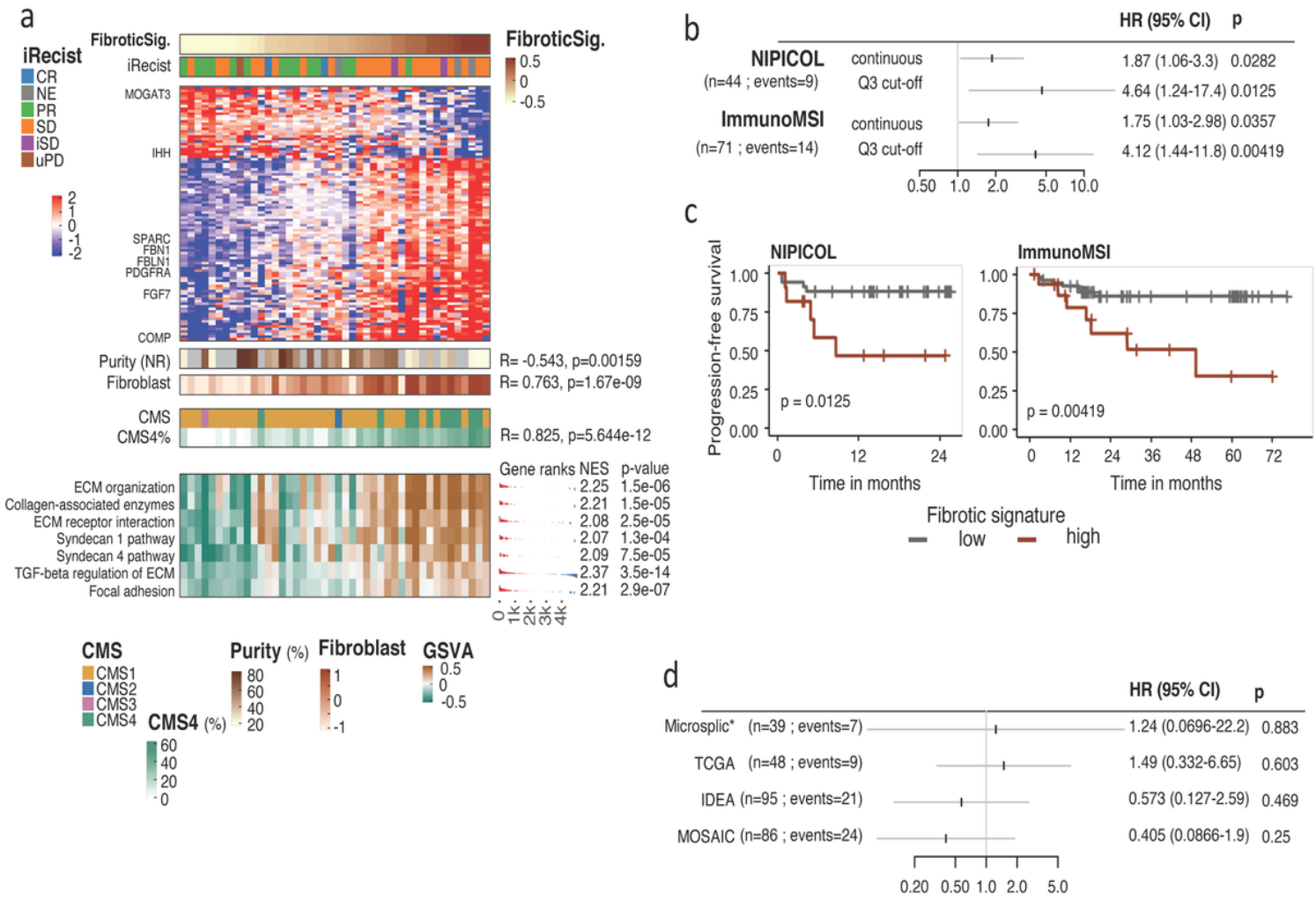

Figure 5

A) Heatmap of the stromal signature, patients (in column) are ordered by the estimated quantification of the stromal ICA signature. iRECIST status of patients [29] are shown along with gene-wise centered expression values of the gene most associated to the component, tumor purity estimated by the non-repeated variant allele frequency, MCPcounter -based fibroblast quantification estimate, the main CMS

(consensus molecular subtype) and the intra-tumoral proportion estimate of CMS4. Pathway-level activity estimate are also shown along with the Gene Set Enrichment Analysis estimates.

B) Univariate association with progression-free survival in C1 or C2 of the continuous score of the signature or of a classification using the third quartile as a threshold (Q3 cut-off).

C) Kaplan-Meier estimates using the third quantile threshold of the stromal signature.

D) Forestplot of the RNA signature with progression-free survival in other cohorts of CRC patients untreated with ICI.

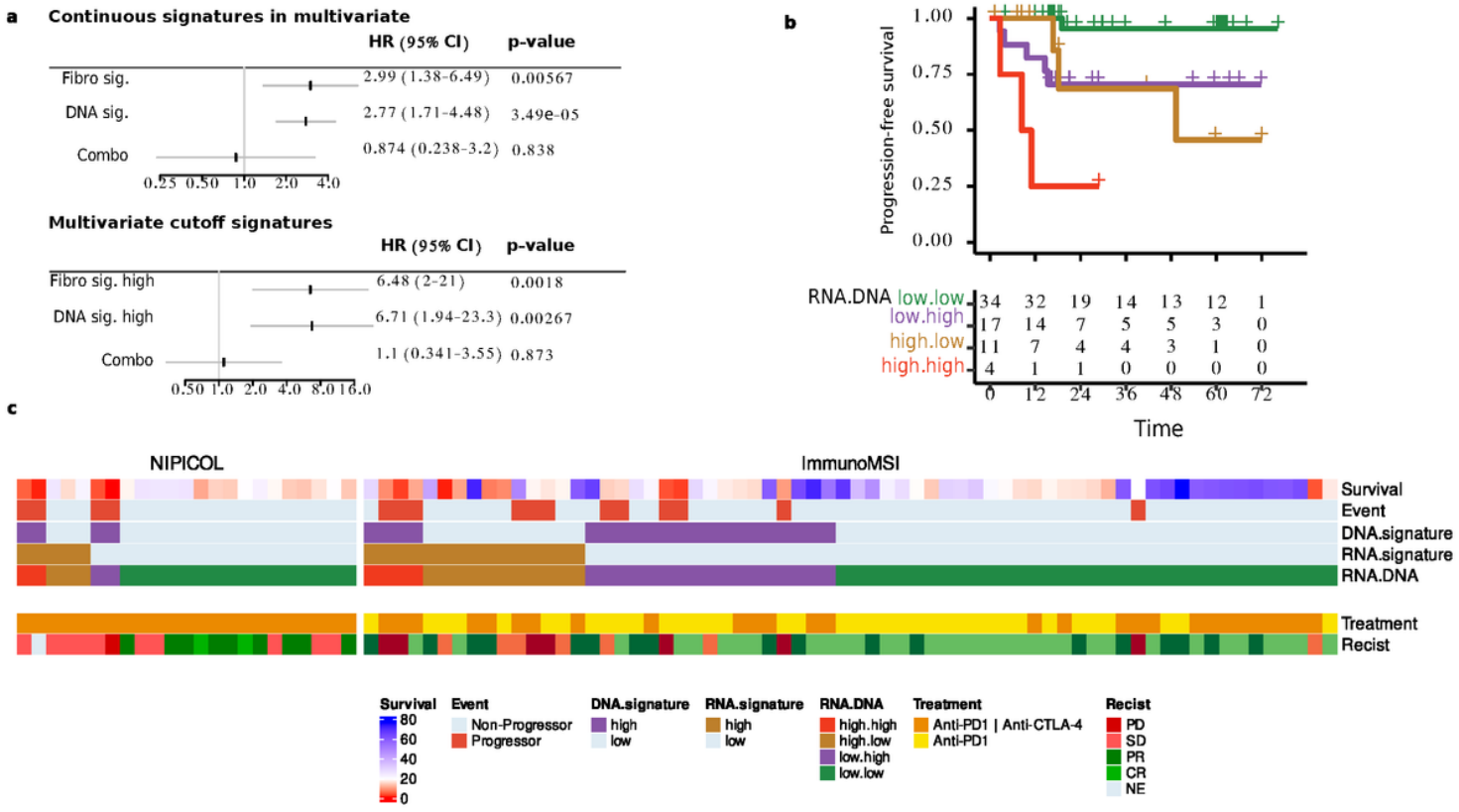

Figure 6

A) Forestplot of the RNA or DNA signatures as well as the combination of both (Combo) considering the continuous value (upper panel) or by discretizing the values (lower panel) of the signatures.

B) Kaplan-Meier estimates of iPFS as a function of the intensity combination of the two signatures. High RNA and DNA signatures are shown in red. Low RNA and DNA signatures are shown in green. High RNA signature and weak DNA signature are shown in orange and low RNA signature and high DNA signature are shown in purple.

C) Heatmap representation, in C1 and C2, of the DNA and RNA models predictions in regard with the patients iPFS, iRECIST status and the treatment (combo-therapy or mono-therapy) [29].

Supplementary Files

This is a list of supplementary files associated with this preprint. Click to download.

- SupplementaryFigureS1.pdf
- SupplementaryFigureS2.pdf
- SupplementaryFigureS3.pdf
- SupplementaryFigureS4.pdf
- SupplementaryFigureS5.pdf
- SupplementaryTableS1.pdf
- SupplementaryTableS2.xlsx
- SupplementaryTableS4.xlsx
- SupplementaryLegends.docx